Nuclear Engineering and Technology 56 (2024) 3255–3267

Contents lists available at ScienceDirect

Nuclear Engineering and Technology

journal homepage: www.elsevier.com/locate/net

Original Article

Whole-core analysis of Watts bar benchmark with three-dimensional MOC code STREAM3D

Murat Serdar Aygul [a], Wonkyeong Kim [a], Deokjung Lee [a,b,*]

[a] Department of Nuclear Engineering, Ulsan National Institute of Science and Technology 50 UNIST-gil, Ulsan, 44919, Republic of Korea
[b] Advanced Nuclear Technology and Services, 406-21 Jonga-ro, Jung-gu, Ulsan, 44429, Republic of Korea

ARTICLE INFO

Keywords:
Reactor physics
Watts bar benchmark
Core design
STREAM3D
3D/DD MOC method

ABSTRACT

This paper presents a high-fidelity simulation of the Organization for Economic Co-operation and Development (OECD) Nuclear Energy Agency (NEA) 3D whole-core Watts Bar benchmark using the UNIST in-house STREAM3D (Steady State and Transient Reactor Analysis code with Method of Characteristics) neutronic code. The benchmark encompasses various whole-core exercises, including single physics problems, multi-physics simulations, and depletion problems. When comparing parameters during the zero-power physics tests, including ITC, DBW, CRW, and criticality tests, STREAM3D results indicate a strong agreement with the measured data and KENO-VI. The comparison with the MC21/CTF code in 3D HFP BOC condition demonstrated strong agreement, with only a 0.42% difference in the normalized radial power distribution, a 0.38 K difference in the RMS of the assembly coolant exit temperature, and a mere 4 ppm difference in CBC.

1. Introduction

Verification and Validation (V&V) are essential requirements for assessing the performance of neutronic computer codes. Evaluating the performance, capacity, and accuracy order of neutronic software developed in the nuclear field plays a crucial role in fulfilling its purposes. Some institutions and organizations make real operational reactor data available, enabling the testing and validation of neutronic software. In line with this objective, the Consortium for Advanced Simulation of Light Water Reactors [1] offers the Virtual Environment for Reactor Applications (VERA) [2] Multi-Physics Core Benchmark. The VERA Core Physics Benchmark Progression Problems covers various 3D whole core problems with detailed structures and materials data. This benchmark publication comprises plant-measured data and results from the high-fidelity Monte Carlo code KENO-VI, providing a reference solution for comparison based on Watts Bar Unit 1 Cycle 1 operation (WB1C1). The Organization for Economic Co-operation and Development (OECD) Nuclear Energy Agency (NEA) [3] has expanded this VERA benchmark publication. Within this benchmark, they have developed 3D reactor core scenarios for Watts Bar Unit 1 Cycle 1-2-3. This paper presents the first three exercises of the OECD/NEA benchmark report, which cover various aspects such as stand-alone scenarios, T/H feedback, and depletion analysis, all derived from WB1C1 [3].

The neutron transport equation can be addressed through deterministic methods as well as the Monte Carlo method. The Monte Carlo method inherently comes with stochastic uncertainties. To reduce these uncertainties and achieve high-fidelity solutions, many neutron histories must be employed. Deterministic code systems, depending on their acceleration techniques, can achieve faster convergence compared to Monte Carlo type codes, providing high-fidelity solutions. However, the discrete ordinate method demands massive computer memory. Therefore, with the rapid advancements in computer technology in recent years, deterministic codes have become more attractive. Advanced methods for solving the 3D neutron transport equations often involve a combination of 2D/1D methods. In this approach, the radial system is typically addressed using a 2D Method of Characteristics (MOC), while the axial system is treated with an SP3 method. While this method is known for providing a good balance between accuracy and computational efficiency, it does have some weaknesses [4]. The first version of this method was first developed and integrated into the DeCART [5]. Subsequently, it was adopted in other code systems like MPACT [6] and nTRACER [7]. On the other hand, the direct 3D MOC method in some code systems, such as OPENMOC [8] is introduced to eliminate the weaknesses in the 2D/1D method. While the direct 3D MOC method has been successfully applied and reduces memory requirements, it often suffers from longer computational times needed to find a convergent

* Corresponding author. Department of Nuclear Engineering, Ulsan National Institute of Science and Technology50 UNIST-gil, Ulsan, 44919, Republic of Korea.
E-mail address: deokjung@unist.ac.kr (D. Lee).

https://doi.org/10.1016/j.net.2024.03.026
Received 8 December 2023; Received in revised form 1 March 2024; Accepted 19 March 2024
Available online 19 March 2024

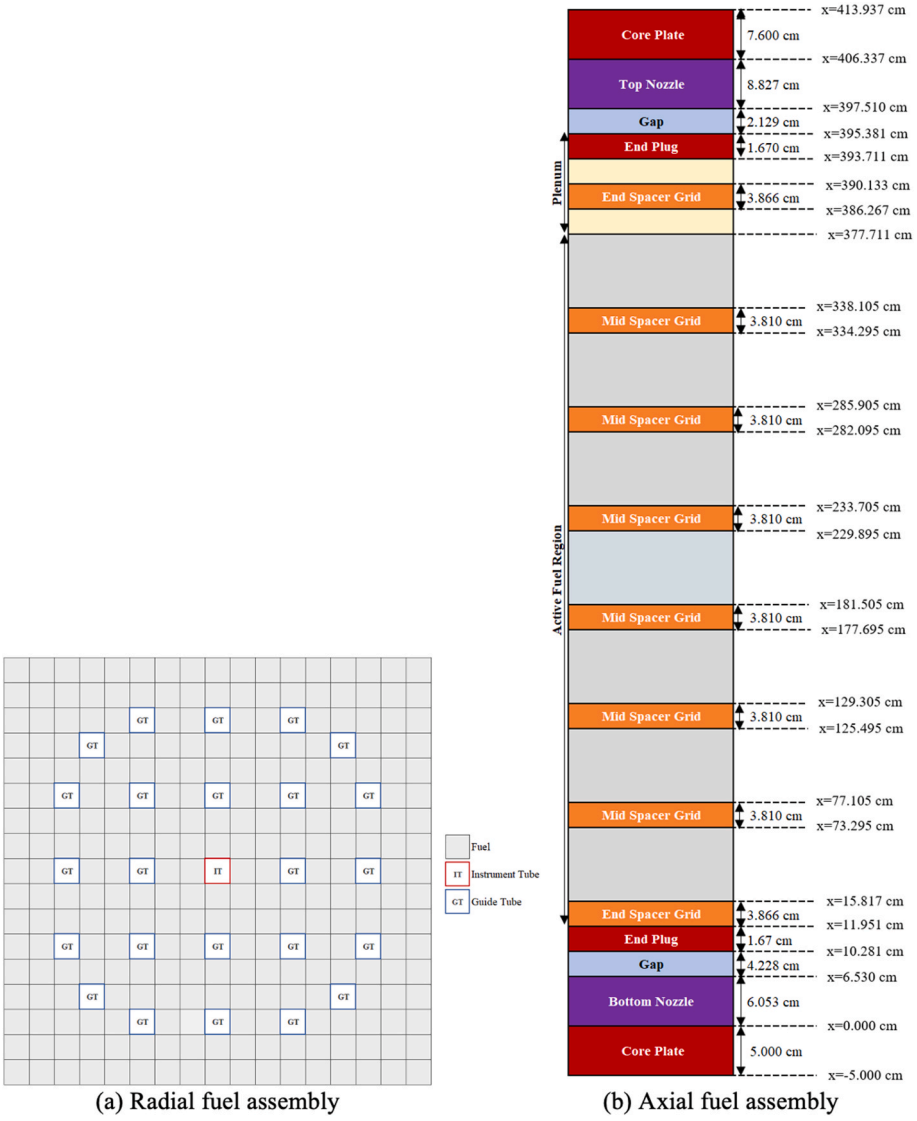

Fig. 1. Fuel assembly radial and axial configuration.

solution. In that scope, the Ulsan National Institute of Science and Technology (UNIST) has been dedicated to developing a deterministic code named STREAM3D (ST3D) to achieve high-fidelity solutions for 3D whole core problems [4]. To address the limitations of conventional methods, a novel approach known as the 3D characteristics/diamond-difference (3D MOC/DD) method has been implemented into the neutron transport analysis code ST3D. The primary objective of this paper is to show the capability of STREAM3D

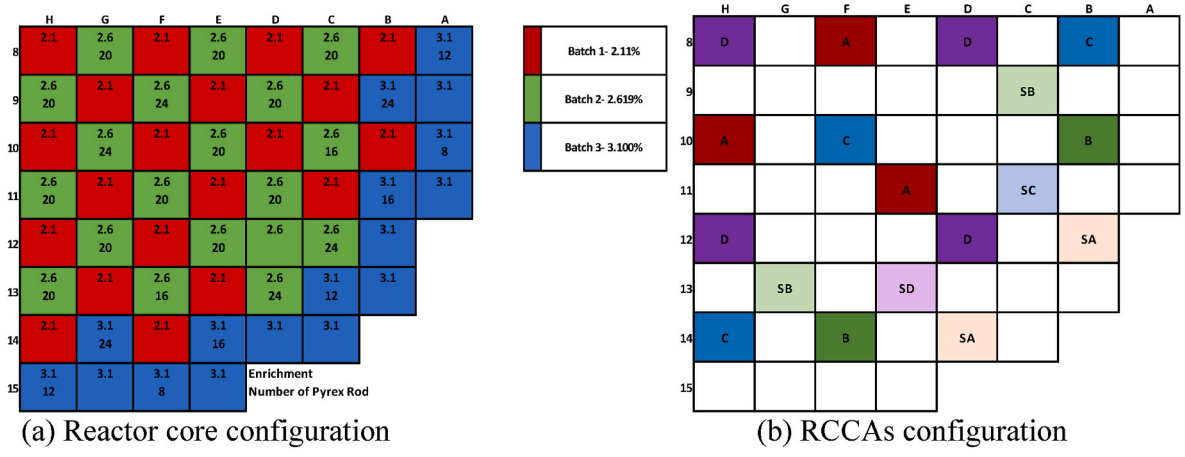

Fig. 2. Watts bar unit 1 cycle 1 reactor core and control bank Configurations.

Table 1
Specification of fuel assembly of WB1C1.

Fuel Rod	Value
Pellet/Gap/Cladding Radius	0.4096 cm/0.4180 cm/0.4750 cm
Pellet/Gap/Cladding Material	UO_2/Helium/Zircolay-4
Fuel Assembly	
Lattice	17 × 17
Assembly Pitch	21.5 cm
Active Fuel Length	365.76 cm
No. Fuel Rods/Guide Tube/Instrument Tube	264/24/1
No. Fuel Assembly	193

Table 2
WB1C1 core and thermal hydraulic specifications.

Parameter	Value
Fuel Density ($\mathbf{g}/cm^3$)	10.257
Fuel Enrichment (%)	2.110/2.619/3.100
Burnable Poison	Pyrex
Rated Core Power (MW_{th})	3411
Inlet Coolant Temperature (K)	565
Inlet Coolant Density ($\mathbf{g}/cm^3$)	0.743
Reactor Pressure (MPa)	15.51320
Reactor Coolant Mass Flow (kg/s)	16591.4009
Cycle Length, EFPDs	441.0
EOC Exposure, GWd/MT	16.939

through various Watts Bar Unit 1 Multi-Physics Multi-Cycle Depletion Benchmark exercises. The structure of this paper is as follows: Section 2 provides an introduction and description of the WB1C1. Section 3 introduces the UNIST deterministic code ST3D and provides a brief overview of the computer codes used as references. Section 4 presents numerical solutions for Exercises 1 to 3 in the benchmark. Finally, Section 5 describes the conclusions and future perspectives.

2. Watts Bar Unit 1 cycle 1 reactor core configuration and specification

Watts Bar Nuclear Power Plant Unit 1 (WB1) is a Pressurized Water Reactor (PWR) designed by Westinghouse and operated by the Tennessee Valley Authority (TVA). It has been in operation since 1996, initially producing 3411 MW of thermal power [9].

Fig. 1 shows the radial and axial configuration of the fuel assembly of WB1C1. Each fuel assembly has a stack height of 365.76 cm and contains 264 fuel rods, 24 guide tubes, and 1 instrumentation tube. Eight spacer grids are used for each assembly to maintain its structural integrity. Fig. 2 shows the initial reactor core loading pattern and layout of reactor cluster rod assemblies (RCCAs) for Cycle 1 of Watts Bar Unit 1, consisting of 193 fuel assemblies and 57 Rod Control Cluster Assemblies (RCCAs), divided into eight separate banks. In this cycle, the reactor core is divided into three enrichment zones containing different levels of U-235 enrichment (2.11%, 2.619%, and 3.10%), and Pyrex burnable absorber cluster assemblies are inserted. The RCCA banks are divided into two groups: control banks (A, B, C, D) for reactor operation and safety banks (SA, SB, SC, SD) for reactor shutdown. An RCCA assemblies are positioned to insert into 24 guide tube locations of the fuel assembly. Control Rod Bank D is the one used to regulate the reactor core during the fuel cycle operation. Additionally, the benchmark provides detailed specifications for ex-core structures such as baffle, core barrel, neutron pad, and reactor vessel. Table 1 and Table 2 provide various core specifications and thermal/hydraulic parameters for WB1C1.

3. Neutronic code systems

In this study, one deterministic code, STREAM3D [4], was employed for our simulations, while two Monte Carlo-type codes, KENO-VI [10] and MC21/CTF [11], were used as reference codes.

3.1. STREAM3D (ST3D) method of characteristics code

ST3D is a neutronic computer code designed for whole-core PWR systems, with a three-dimensional method of characteristics neutron transport analysis. This code is aimed at addressing limitations found in conventional 3D neutron transport analysis methods. Therefore, ST3D has implemented a new approach called the 3D characteristics/diamond-difference (3D MOC/DD) method in its neutron transport analysis. In the diamond-difference scheme, the source in the axial direction is homogenized into a pin-cell square as a function of the source region and neutron streaming angle. In other words, axial source regions occupy the radial MOC solver. Therefore, this method does not require an axial solver. Consequently, each plane is axially connected with a linear order diamond difference scheme, which limits the axial mesh height. Hence, it is recommended to use a mesh height of less than 3 cm to obtain high-fidelity solutions [4]. As a result, ST3D employs a higher number of axial planes compared to 2D/1D methods. ST3D is a sophisticated and comprehensive code system that encompasses a wide array of features and libraries to make a detailed analysis of neutron transport and reactor physics calculations. One of its key attributes is the multi-group cross-section and resonance integral library. This library includes data from various nuclear databases, such as ENDF/B-VII.0, ENDF/B-VII.1, ENDF/B-VIII.0, and JENDL-4.0. ST3D has 72 energy groups from 1×10^{-5} eV to 20 MeV and 39 resonance energy groups between 0.3 eV and 24,780 eV. The code system further enhances its capabilities by offering a resonance up scattering correction factor feature, implemented through the Monte Carlo code MCS [12]. It employs the Pin-Based Pointwise Slowing Down Method [13], to mitigate the effects of resonances in the neutron spectrum as a resonance treatment method. OPENMPI/MPI hybrid parallelization is implemented in ST3D, enabling efficient and scalable simulations on modern high-performance computing clusters. To accelerate the code system further, ST3D utilizes the Coarse Mesh Finite Difference (CMFD) acceleration technique, speeding up fission source convergence in neutron transport calculations. Moreover, it uses the inflow transport corrections method [14] to handle anisotropic scattering effects. The ST3D library is a comprehensive tool for performing depletion calculations, offering data on approximately 1300 nuclides. It has decay and yield libraries derived from ENDF/B-VII.0 and VII.1, ensuring the accuracy of its calculations. ST3D utilizes the Chebyshev Rational Approximation Method (CRAM) method for depletion calculation, which is known for its efficiency and precision in solving the Bateman equations. In addition, ST3D can provide thermal-hydraulic feedback with its inner TH1D module which models one single-phased closed channel per pin [15]. To conclude, ST3D is capable of conducting a comprehensive analysis of the PWR-type core, which is essential for ensuring reactor safety and stability [4]. Fig. 3 shows the explicit axial and radial material configuration of the WB1C1 reactor core modeled in ST3D.

3.2. KENO-VI

KENO-VI [10], a widely utilized 3D Monte Carlo code for neutron transport and radiation shielding analysis, is an integral component of the SCALE (Standardized Computer Analysis for Licensing Evaluation) [16] code system, developed by the Oak Ridge National Laboratory (ORNL) in the United States. It serves as one of the primary criticality safety analysis tools within the SCALE [16] framework. It is widely adopted by the United States Nuclear Regulatory Commission (NRC) to facilitate standardized analyses and evaluations of nuclear facilities. All KENO-VI solutions are obtained in Ref. [2].

3.3. MC21/CTF

MC21 [11] is a novel Monte Carlo code for simulating neutron and photon transport. Its development is a collaborative effort between the Knolls Atomic Power Laboratory and the Bettis Atomic Power

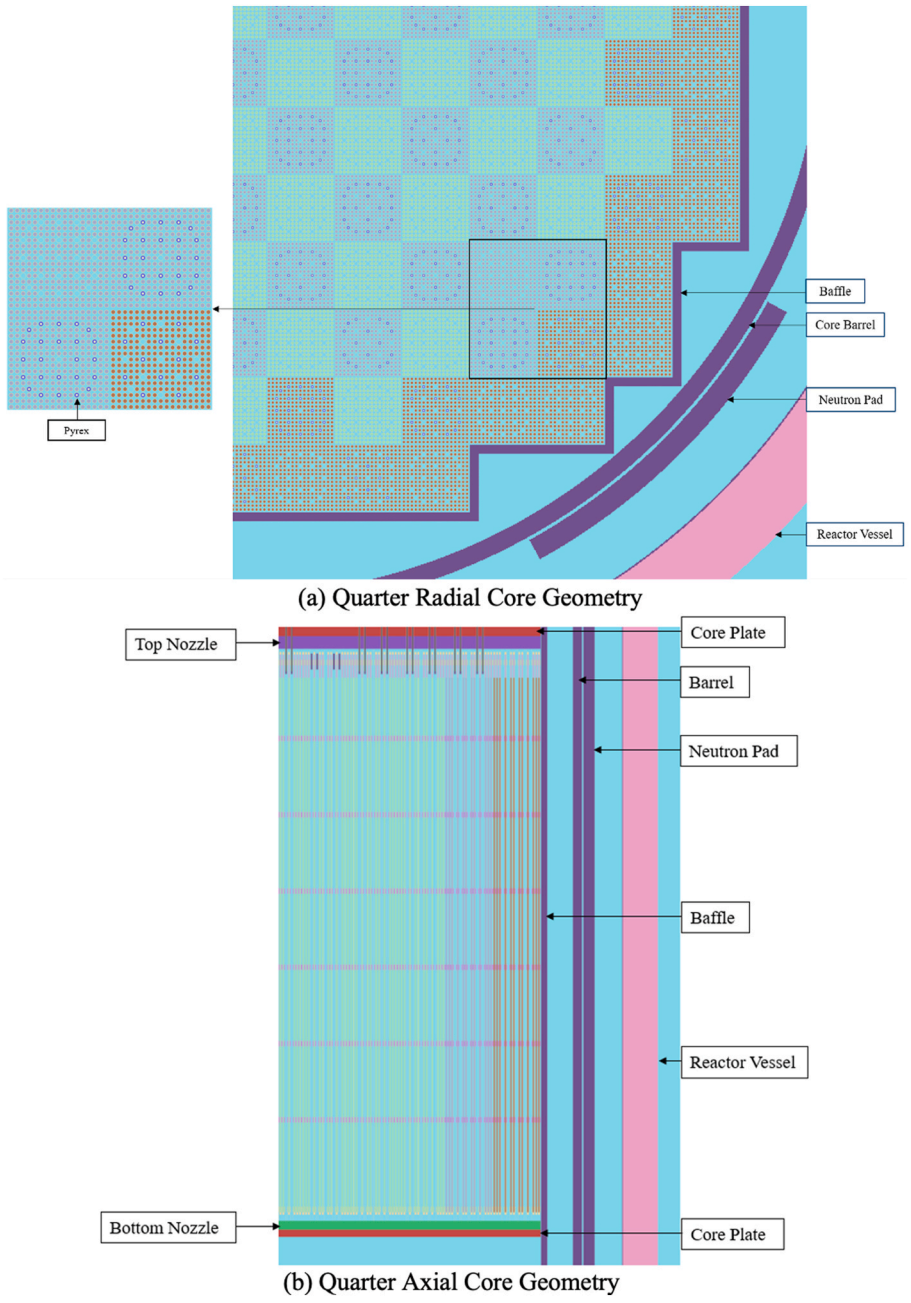

Fig. 3. Radial and axial material configuration of Watts Bar Unit 1 core in STREAM3D.

Laboratory. MC21 aims to transform the Monte Carlo method from a benchmarking tool into a primary design tool. CTF (Coolant-Boiling in Rod Arrays - Three Fluids) [17] is a widely used thermal-hydraulic subchannel code in the field of nuclear engineering and reactor safety analysis. It is used for simulating the behavior of coolant (typically water) as it flows through a nuclear reactor's fuel assembly. MC21 and CTF are coupled to provide a comprehensive analysis of nuclear reactor behavior.

4. Numerical results

The following section will present numerical results with ST3D in different cases; single physics problems, steady-state nominal operation conditions, and whole-core depletion. All necessary data related to reactor core specification, configuration, and desired outputs are sourced from the OECD/NEA benchmark publication [3]. However, since this publication does not include any neutronic code solutions as references or plant-measured data, KENO-VI solutions and plant-measured data obtained from the CASL benchmark publication are used for comparison [2]. The reactor core is modeled with quarter core symmetry, including instrument tubes. Cross-section reconstruction was made using ENDF/B-VII.I. It is worth noting that KENO-VI solutions were generated using ENDF/B-VII.0. Therefore, library differences between the two codes can potentially cause some additional small differences in the solutions. In the simulations performed by ST3D, MOC ray parameters are used for all exercises as follows: a ray spacing of 0.05 cm, 48 azimuthal angles, and 6 polar angles. These parameters are set as default in ST3D due to their demonstrated efficacy in achieving high-fidelity results [4,18]. Equation (1) and Equation (2) are employed for determining the differences between multiplication factors, denoted as k_{eff}, and discrepancies in pcm or various parameters. Relative error difference and root mean square error used for power distribution are

Table 3
Reactivity differences at criticality tests.

Boron Concentration (ppm)	Bank D Position (Withdrawn Steps)	Fully Inserted Bank	KENO-VI (k_{eff})	ST3D (k_{eff})	Difference (pcm)
1285	167	–	0.99990 ± 0.00001	0.99862	−128
1291	230	–	1.00032 ± 0.00001	0.99904	−128
1170	97	Bank A	0.99880 ± 0.00001	0.99751	−129
1170	113	Bank B	0.99936 ± 0.00001	0.99804	−132
1170	119	Bank C	0.99904 ± 0.00001	0.99776	−128
1170	18	Bank D	0.99908 ± 0.00001	0.99782	−126
1170	69	Bank SA	0.99902 ± 0.00001	0.99767	−135
1170	134	Bank SB	0.99932 ± 0.00001	0.99809	−123
1170	71	Bank SC	0.99898 ± 0.00001	0.99771	−127
1170	71	Bank SD	0.99898 ± 0.00001	0.99771	−127

given in Equation (3) and Equation (4), respectively.

$$k_{eff}\ \text{difference [pcm]} = \left(1/k_{eff,S} - 1 \Big/ k_{eff,R}\right) \times 10^5 \quad (1)$$

$$\text{The difference in pcm or parameters} = S - R \quad (2)$$

$$\text{Relative Error Difference } [\%] = \frac{S-R}{R} \times 100 \quad (3)$$

$$\text{Root Mean Square Error (RMS) } [\%] = \left(\sqrt{\frac{\sum_{k=1}^{N}(S_k - R_k)^2}{N}}\right) \times 100 \quad (4)$$

where S is the solution provided by ST3D and R is the reference solution, which refers to measured data, KENO-VI, and MC21/CTF.

4.1. Exercise 1: validation of cycle 1 stand-alone 3-D neutronics model at hot zero power conditions

This exercise is designed to calculate various important parameters related to the beginning of Cycle 1 (BOC) start-up of WB1C1, specifically focusing on the Zero Power Physics Testing (ZPPT). All fuel assemblies are at the beginning of life conditions, and the reactor is the hot zero power isothermal conditions. The reference results for comparison in this exercise are taken by benchmark documentation for validation. The exercise consists of several ZPPT tasks, which include criticality tests, determining the worth of control element assemblies (CEAs), calculating the differential boron worth (DBW), and evaluating the isothermal temperature coefficient (ITC). First, a set of ten criticality tests was conducted with given boron concentration and Bank D positions.

Table 3 presents a comparison between ST3D, and the benchmark results obtained from the high-fidelity Monte Carlo code, KENO-VI [2]. This comparison provides insights into the accuracy of ST3D. Notably, ST3D consistently shows a high level of accuracy, with discrepancies typically limited to within ±130 pcm for all criticality test cases. The reactor core was segmented into a range of 180–190 axial planes for all given scenarios. The reason for employing different numbers of axial planes for the same reactor core is due to the usage of different control rod locations in each case. In other words, since the material composition in the axial direction changes, the number of axial planes is also subject to change.

The total reactivity worth for each control bank is calculated individually by fully inserting them into the reactor core under all rod out (ARO) conditions, maintaining a constant 1170 ppm boron concentration. A comparison of control rod worth between ST3D and plant-measured data as well as KENO-VI is shown in Table 4 [2]. The corresponding CRWs are also compared in Fig. 4. ST3D provided a good prediction of the initial criticality, with differences of 128 pcm compared to measured data and 138 pcm compared to KENO-VI. It slightly underestimated the initial criticality.

In general, ST3D tends to predict control rod worth values that are slightly higher, typically within a range of ±50 pcm compared to plant-measured data. The most significant deviation is observed with Bank A, showing a difference of 54 pcm. On the other hand, when comparing ST3D to KENO-VI, there is great agreement, with differences within only ±5 pcm. The isothermal temperature coefficient (ITC) and differential boron worth (DBW) at ARO conditions of ST3D are compared with measured data and KENO-VI, and the results are presented in Table 4. The DBW calculations were performed at 565 K with boron concentrations of 1291 ppm and 1170 ppm. ST3D demonstrates remarkable agreement, with differences against measured data and KENO-VI within the range of 0 ppm/pcm to 0.6 ppm/pcm. Similarly, for ITC calculations, involving two temperature points at 1291 ppm boron concentration (560 K and 570 K), ST3D consistently shows strong agreement, with differences ranging from −1.17 pcm/°F to −0.16 pcm/°F when

Table 4
CRW, ITC, and DBW comparison.

Test Cases	Measured Data	KENO-VI	ST3D	Difference vs Measured Data	Difference vs KENO-VI
Initial Criticality	1.0000	0.99990 ± 0.00001	0.99862	−138	−128
Rod Worth(pcm)					
Bank Name					
A	843	898 ± 2	897	54	−1
B	879	875 ± 2	879	0	4
C	951	984 ± 2	984	33	0
D	1342	1386 ± 2	1386	44	0
SA	435	447 ± 2	450	15	3
SB	1056	1066 ± 2	1066	10	0
SC	480	499 ± 2	498	18	−1
SD	480	499 ± 2	498	18	−1
TOTAL	6467	6654 ± 6	6658	191	4
DBW(pcm/ppm)	−10.77	−10.21	−10.21	0.56	0
ITC (pcm/°F)	−2.17	−3.18	−3.34	1.17	0.16

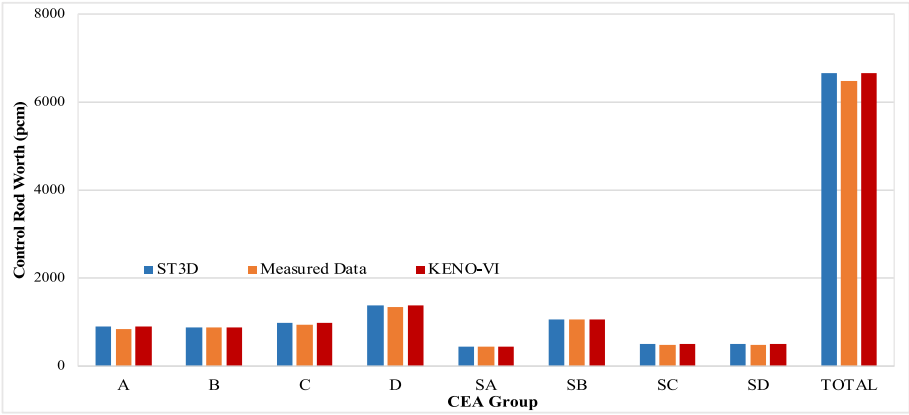

Fig. 4. Control rod worth comparison.

	H	G	F	E	D	C	B	A
8	0.949 0.945 0.37%	0.919 0.919 0.00%	1.018 1.014 0.40%	0.985 0.985 0.04%	1.065 1.061 0.38%	1.048 1.049 -0.09%	1.084 1.083 0.09%	0.793 0.798 -0.64%
9	0.919 0.919 0.01%	0.997 0.993 0.37%	0.908 0.908 0.05%	1.082 1.077 0.46%	1.047 1.047 0.00%	1.162 1.158 0.35%	1.065 1.068 -0.28%	0.907 0.912 -0.53%
10	1.018 1.014 0.40%	0.908 0.907 0.06%	1.064 1.060 0.38%	1.041 1.040 0.10%	1.175 1.170 0.43%	1.152 1.152 0.00%	1.104 1.102 0.18%	0.805 0.809 -0.49%
11	0.985 0.984 0.07%	1.082 1.077 0.46%	1.041 1.040 0.10%	1.162 1.156 0.52%	1.085 1.085 0.00%	1.151 1.148 0.26%	1.050 1.053 -0.28%	0.659 0.663 -0.59%
12	1.065 1.061 0.38%	1.047 1.046 0.10%	1.175 1.170 0.43%	1.085 1.085 0.00%	1.237 1.236 0.08%	0.897 0.899 -0.23%	0.945 0.950 -0.54%	
13	1.048 1.048 0.00%	1.162 1.158 0.35%	1.152 1.152 0.00%	1.151 1.148 0.26%	0.897 0.899 -0.21%	0.913 0.917 -0.47%	0.630 0.635 -0.82%	
14	1.084 1.082 0.19%	1.065 1.068 -0.28%	1.104 1.101 0.27%	1.050 1.053 -0.28%	0.945 0.949 -0.46%	0.630 0.635 -0.79%		
15	0.793 0.797 -0.51%	0.907 0.911 -0.41%	0.805 0.808 -0.39%	0.659 0.662 -0.51%				

KENO-VI STREAM3D Rel. Diff. (%)	
Max Diff.	0.52%
Min Diff.	-0.82%
RMS	0.36%

Fig. 5. Normalized radial assembly power distribution comparison for initial criticality case.

compared to measured data and KENO-VI, respectively.

In the benchmark publication, the initial criticality case is given as 1285 ppm and 167 steps withdrawn Bank D position. KENO-VI provides assembly-wise radial power distribution and 1D core axial distribution [2]. These data are generated by ST3D and compared with KENO-VI [2] as shown in Figs. 5–6. The normalized power distribution in ST3D closely corresponds with the values obtained from KENO-VI, resulting in corresponding RMS differences of merely 0.36%. Furthermore, the maximum difference observed is less than 1% across all assembly cases, signifying great agreement. Both code systems consistently show a very similar power distribution shape across the active core in the 1D axial power distribution, except for the first spacer grid location.

The reactivity impact of Bank D on the reactor core is subject to thorough analysis, as this bank plays a significant role in maintaining criticality with the soluble boron concentration in the coolant during the fuel cycle. In Figs. 7–8, the differential worth curve, integral worth curve, and step worth of Bank D are presented. These data were calculated using a withdrawal process of 10% (23 steps) at 565 K and 1170 ppm boron concentration, while all other control banks were fully withdrawn. ST3D shows a high level of agreement with KENO-VI [2]. ST3D demonstrates remarkable consistency, with differences typically falling within around ±0.2 pcm for step worth calculations and ±5 pcm for Integral Rod Worth (IRW) when compared to KENO-VI. As a last part of this exercise, a comprehensive overview of the parameters and run-time metrics for the initial criticality condition is given as shown in Table 5. The simulation used 183 axial source planes and 79 axial material planes, with 144 source planes and 54 material planes in the active regions, respectively. The number of total flat source regions used in the simulation is 180,521,265. Computationally, the simulation utilized 264 computing cores, with a total run-time of 3.53 h, corresponding to 931.32 core-hours, and requiring 1.896 TB of memory.

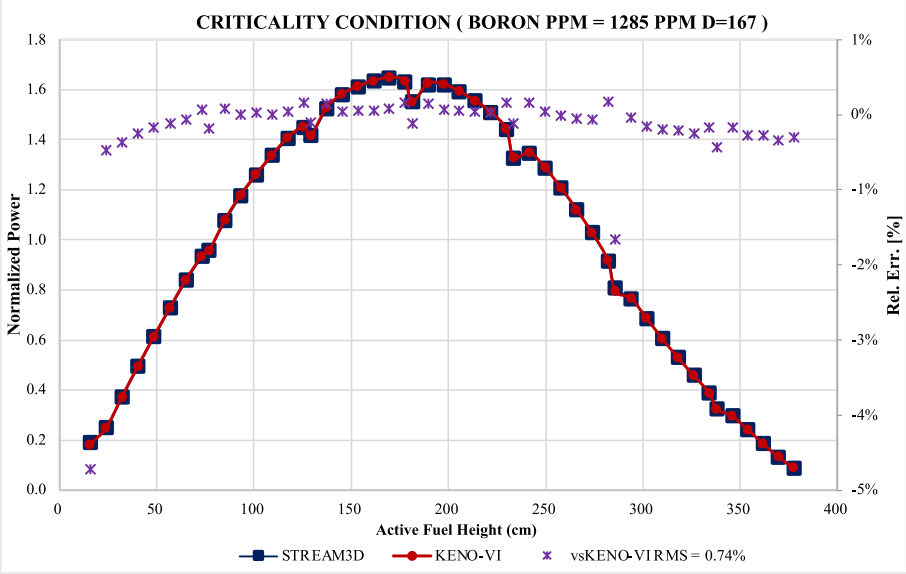

Fig. 6. 1D core axial power distribution comparison at initial criticality case.

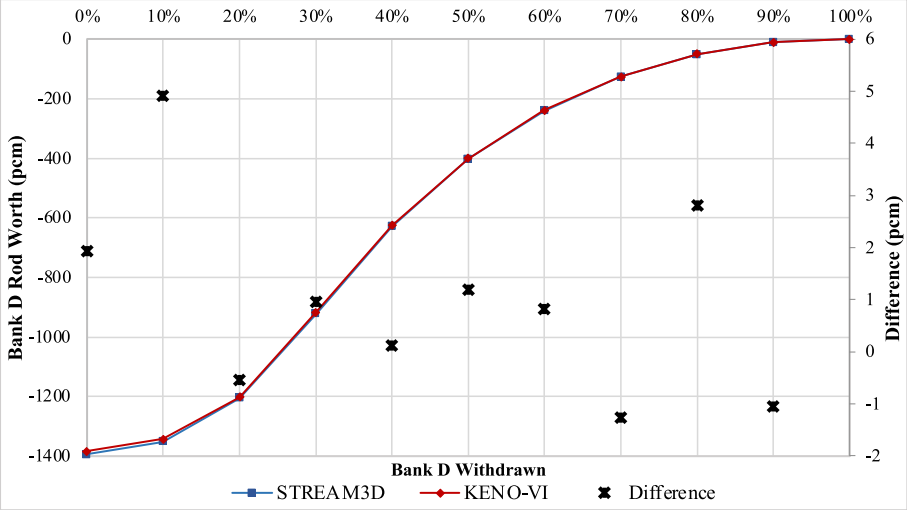

Fig. 7. Control Bank D integral curve comparison.

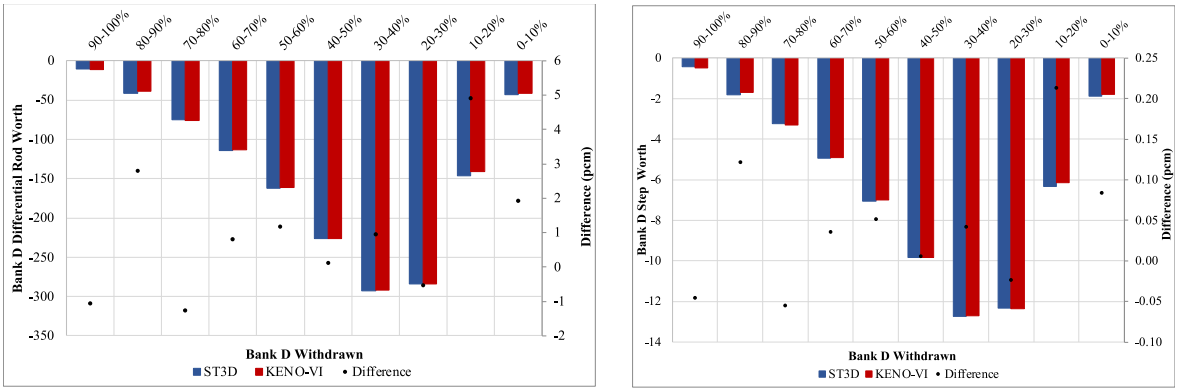

Fig. 8. Control Bank D differential and step worth comparison.

Table 5
Calculation parameters and run-time for the initial criticality condition.

Parameter	Value
Methods	3D MOC/DD
Ray spacing/# of azimuthal Angles/# of polar angles	0.05 cm/48/6
Core Symmetry	Quarter
# of energy Groups	72
# of axial source planes/# of axial source in active regions	183/144
# of axial material planes/# of axial material in active regions	79/54
# of source regions	180,521,265
Computing cores[a]	264
Run-time (hours)	3.53
Run-time (core-hours)	931.32
Total Memory (TB)	1.896

[a] Intel(R) Xeon(R) Gold 6242 R CPU @ 3.10 GHz.

Table 6
Critical Boron Concentration comparison at BOC HFP condition [ppm].

Code System	CBC	Differences
STREAM3D-TH1D	858.6	–
MC21-CTF	854.5	−4.1

4.2. Exercise 2: Verification of cycle 1 multi-physics steady-state model for HFP conditions

The target of this exercise is to perform a steady-state multi-physics simulation of Watts Bar Unit 1 Cycle 1 (WB1C1) under normal operating conditions. This simulation aims to analyze the impact of the concentration of xenon and thermal-hydraulic feedback on neutronics in both the fuel and coolant. It is important to note that in this section of the simulation, only Bank D is partially inserted into the reactor core, and it has been withdrawn in 215 steps as part of the operational procedure. Equilibrium xenon and critical boron concentration (CBC) search features are implemented throughout the reactor core in ST3D. Additionally, for thermal feedback, it is coupled with the inner TH1D module [15]. The core geometry has been divided into 181 axial meshes, and, to improve solution accuracy, the Pyrex burnable absorber regions have been segmented into three rings to ensure more precise results.

Given the absence of data within the benchmark publication report concerning assembly radial power distributions and the assembly coolant exit temperature profiles, as a benchmark recommendation, MC21-CTF solutions were utilized as reference data for this part of the benchmark analysis. The MC21/CTF code has utilized many neutron histories and strategies to generate high-fidelity solutions with low uncertainties [9].

Table 6 presents the estimated CBC values under Hot Full Power (HFP) conditions, estimated by MC21-CTF [9] and ST3D-TH1D. ST3D-TH1D shows a slight overestimation of CBC compared to MC21-CTF, with differences of about 4 ppm.

Figs. 9–10 demonstrate normalized assembly-wise radial power distribution and assembly coolant exit temperature distribution comparison between ST3D and MC21 [9]. RMS error for normalized radial power distribution of ST3D-TH1D agrees well with that of MC21-CTF, with RMS differences of only 0.42%. ST3D-TH1D demonstrates maximum and minimum differences of typically less than 1% across all assemblies. RMS differences in the assembly coolant channel exit temperature to 0.38 Celsius. While the MC21 employs a sophisticated thermal-hydraulic module for its feedback calculations, the ST3D shows remarkable agreement across the assemblies, accurately predicting temperature differentials of less than approximately 1 Celsius across the entire core. It's worth noting that in low-enrichment fuel assembly zones, ST3D-TH1D tends to predict lower power values. Conversely, higher predictions are observed in high-enrichment fuel assemblies. Due to the absence of available data regarding 1D axial power, fuel, and temperature profiles produced by MC21/CTF, only ST3D data is provided as shown in Figs. 11–12, and comparison cannot be performed. In this part, spacer grids are treated as separate mesh regions, and the fuel regions outside the fuel spacer grid are divided into approximately 8 cm axial regions as specified in the given benchmark [3].

Table 7 summarizes the calculation parameters and run-time at the beginning of the cycle (BOC) hot full power (HFP) condition. In this exercise, ST3D used 181 axial source planes, with 143 in active regions, and 78 axial material planes, with 54 in active regions. The simulation comprised a total of 179,553,267 flat source regions. The computation was distributed across 112 computing cores, achieving convergence in 16.52 h, equivalent to 1849.82 core hours. The total memory usage was 1.809 TB. These parameters provide essential insights regarding computational efficiency and accuracy at BOC HFP conditions for STREAM3D.

	H	G	F	E	D	C	B	A
8	1.118 1.110 0.70%	1.030 1.028 0.18%	1.116 1.108 0.70%	1.056 1.055 0.08%	1.157 1.151 0.51%	1.053 1.054 -0.11%	1.049 1.047 0.18%	0.756 0.760 -0.56%
9	1.030 1.028 0.18%	1.108 1.101 0.62%	0.983 0.982 0.07%	1.148 1.141 0.60%	1.080 1.079 0.08%	1.155 1.152 0.25%	1.012 1.016 -0.41%	0.856 0.860 -0.42%
10	1.115 1.108 0.62%	0.983 0.982 0.07%	1.131 1.125 0.52%	1.074 1.074 -0.01%	1.184 1.180 0.33%	1.121 1.122 -0.10%	1.055 1.054 0.08%	0.765 0.769 -0.55%
11	1.056 1.055 0.08%	1.147 1.141 0.51%	1.074 1.074 -0.01%	1.180 1.174 0.50%	1.077 1.079 -0.20%	1.118 1.116 0.17%	0.987 0.991 -0.45%	0.634 0.638 -0.60%
12	1.157 1.151 0.51%	1.079 1.079 -0.01%	1.185 1.180 0.41%	1.078 1.079 -0.11%	1.238 1.236 0.15%	0.865 0.869 -0.48%	0.891 0.896 -0.54%	
13	1.054 1.054 -0.01%	1.156 1.152 0.33%	1.122 1.122 -0.01%	1.119 1.116 0.26%	0.865 0.869 -0.48%	0.866 0.870 -0.51%	0.607 0.613 -0.95%	
14	1.049 1.047 0.18%	1.013 1.016 -0.31%	1.057 1.054 0.27%	0.988 0.991 -0.35%	0.892 0.896 -0.43%	0.608 0.613 -0.79%		
15	0.756 0.760 -0.56%	0.857 0.860 -0.30%	0.765 0.769 -0.55%	0.634 0.638 -0.60%				

MC21-CTF
ST3D-TH1D
Rel. Diff. (%)

Max. Diff.	0.70%
Min. Diff.	-0.95%
RMS	0.42%

Fig. 9. Radial assembly power comparison at BOC HFP condition.

	H	G	F	E	D	C	B	A
8	330.900 330.550 -0.35	327.400 328.050 0.65	330.800 330.450 -0.35	328.200 328.850 0.65	332.100 331.750 -0.35	328.200 328.850 0.65	328.900 328.650 -0.25	318.500 319.250 0.75
9	327.400 328.050 0.65	330.500 330.250 -0.25	325.900 326.550 0.65	331.800 331.450 -0.35	329.000 329.650 0.65	332.200 331.750 -0.45	326.600 327.750 1.15	321.900 322.550 0.65
10	330.800 330.450 -0.35	325.900 326.550 0.65	331.300 330.950 -0.35	328.800 329.450 0.65	333.000 332.650 -0.35	330.300 330.950 0.65	329.200 328.850 -0.35	318.700 319.550 0.85
11	328.200 328.850 0.65	331.800 331.450 -0.35	328.800 329.450 0.65	332.900 332.450 -0.45	329.100 329.650 0.55	331.000 330.750 -0.25	326.000 326.850 0.85	314.500 315.050 0.55
12	332.100 331.750 -0.35	329.000 329.650 0.65	333.000 332.650 -0.35	329.100 329.650 0.55	334.200 334.350 0.15	322.500 323.050 0.55	323.000 323.750 0.75	
13	328.200 328.850 0.65	332.200 331.750 -0.45	330.300 330.950 0.65	331.100 330.750 -0.35	322.600 323.050 0.45	322.100 323.050 0.95	313.600 314.250 0.65	
14	328.900 328.650 -0.25	326.700 327.750 1.05	329.200 328.850 -0.35	326.000 326.850 0.85	323.100 323.750 0.65	313.600 314.250 0.65		
15	318.500 319.250 0.75	321.900 322.550 0.65	318.800 319.550 0.75	314.500 315.050 0.55				

MC21-CTF ST3D-TH1D Abs. Diff.	
Max. Diff.	0.24
Min. Diff.	-0.45
RMS	0.38

Fig. 10. Radial assembly coolant exit temperature comparison at BOC HFP condition.

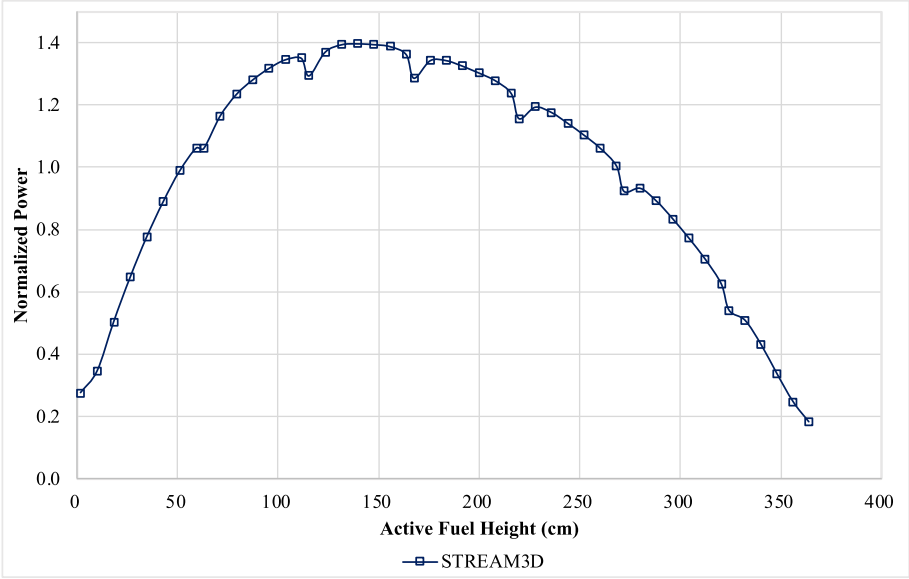

Fig. 11. 1D core normalized power distribution at BOC HFP.

4.3. Exercise 3: validation of cycle 1 depletion model

This exercise aims to predict the depletion of WB1C1 fuel and burnable absorbers, along with the estimation of CBC values throughout the fuel cycle. In PWR-type reactors, criticality is primarily maintained using boron solution in the reactor coolant system with control banks. Therefore, making a good CBC prediction is a pivotal aspect of evaluating T/H feedback and neutronic code performance during the fuel cycle. The core geometry is axially subdivided into over 220 axial meshes, and to enhance solution accuracy, Pyrex burnable absorber regions have been discretized into three rings to achieve more accurate results. A predictor-corrector algorithm was implemented in the depletion simulation. Thermal feedback is provided by the inner TH1D module. The equilibrium xenon and critical boron concentration (CBC) have been applied throughout the reactor core geometry. As the current version of ST3D cannot change the control position and inlet temperature during a simulation, when the control rod position and inlet temperature change, the simulation for the respective burnup step is restarted by following the control position and inlet temperature.

The ST3D depletion model has 30 burnup points as given in the benchmark [3]. However, the OECD/NEA benchmark report has not provided any CBC solutions for this exercise. Instead, plant-measured data from the CASL report were used for comparison, which offers a more detailed power profile, including 93 CBC measurements throughout the cycle [2]. Although a direct comparison between CASL and OECD/NEA depletion points may not be feasible in this exercise, the general trend of ST3D solutions can be observed, as shown in Fig. 13. Even though there are slight disparities in the CBC values during the first half of depletion, the latter half demonstrates better agreement with plant-measured data. Following this part, the active core region is

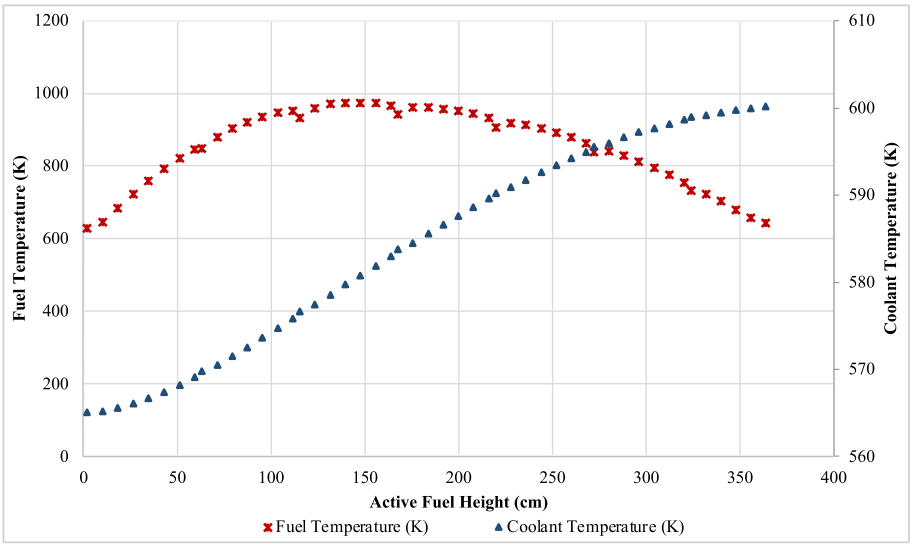

Fig. 12. 1D core fuel and coolant temperature profile at BOC HFP.

Table 7
Calculation parameters and run-time at BOC HFP condition.

Parameter	Value
Methods	3D MOC/DD
Ray spacing/# of azimuthal Angles/# of polar angles	0.05 cm/48/6
Core Symmetry	Quarter
# of energy Groups	72
# of axial source planes/# of axial source in active regions	181/143
# of axial material planes/# of axial material in active regions	78/54
# of source regions	179,553,267
Computing Cores	112
Run-time (hours)[a]	16.52
Run-time (core-hours)	1849.82
Total Memory (TB)	1.809

[a] Intel(R) Xeon(R) Gold 6242 R CPU @ 3.10 GHz.

divided into equal parts with a 6.096 cm axial thickness to generate 1D core data as specified in the benchmark [3]. Fig. 14 shows the assembly-wise radial normalized power distribution in four burnup points specified in the benchmark [3]. As burnup increases in a nuclear reactor, the power distribution is shifted from the inner to the outer regions of the reactor core. This shift primarily arises from the higher consumption of fissile material in the fuel assemblies located in the central regions compared to those in the outer regions. However, as burnup increases and fissionable material is depleted in these central regions, it leads to a decrease in power production within the central fuel assembly regions. In contrast, fissionable material is slowly depleted, resulting in an increase in the relative fission rates at the core periphery and relatively higher power levels by the end of the cycle. A similar pattern is observed in the axial power distribution, where fission rates around the mid-regions decrease rapidly, resulting in a decrease in power distribution in this region. In contrast, the fission rates at the top and bottom regions of the active core gradually rise, leading to a gradual increase in power from the BOC to the EOC as shown in Fig. 15.

Fig. 16 represents the axial temperature profiles of both the 1D core fuel and the coolant at four different burnup points. The fuel temperature is directly linked to the fission rates within the fuel rod, and therefore, the shape of the fuel temperature profile reflects the power distribution based on the power level of the reactor core. Meanwhile, the coolant temperature consistently increases along the axial direction in response to the heat generated by the fuel rod and stored in the coolant. The changes in average fuel temperature, average coolant temperature,

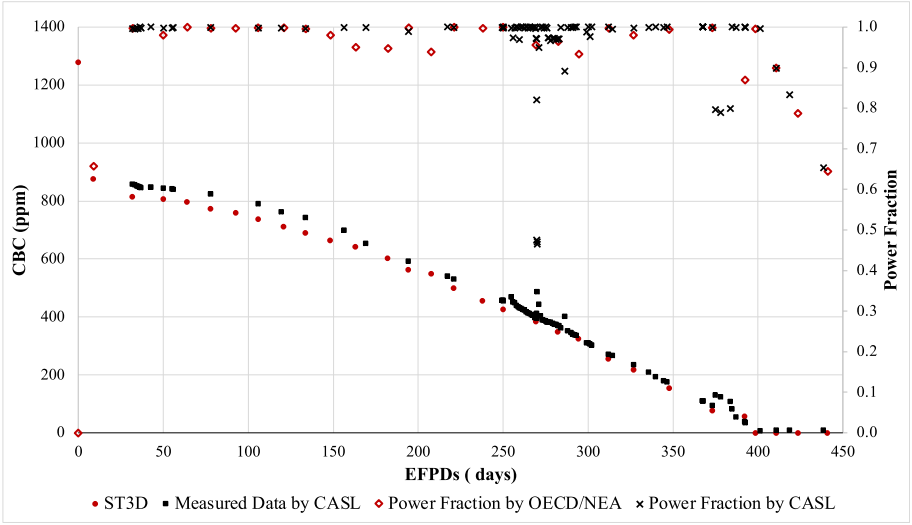

Fig. 13. CBC and power fraction values during WB1C1.

	H	G	F	E	D	C	B	A	
8	1.181	1.128	1.168	1.129	1.168	1.078	1.009	0.722	64 EFPD
	1.163	1.188	1.156	1.174	1.128	1.106	0.977	0.721	221 EFPD
	1.072	1.122	1.081	1.123	1.071	1.107	0.999	0.783	398 EFPD
	1.060	1.103	1.059	1.108	1.069	1.107	1.003	0.793	441 EFPD
9	1.128	1.168	1.077	1.178	1.126	1.132	1.000	0.798	
	1.188	1.159	1.156	1.148	1.154	1.085	1.022	0.768	
	1.122	1.081	1.115	1.081	1.120	1.064	1.076	0.811	
	1.103	1.058	1.097	1.063	1.111	1.059	1.089	0.819	
10	1.168	1.077	1.171	1.135	1.177	1.118	0.999	0.716	
	1.156	1.156	1.151	1.171	1.127	1.113	0.952	0.699	
	1.081	1.115	1.082	1.125	1.079	1.107	0.972	0.754	
	1.059	1.097	1.061	1.111	1.067	1.105	0.976	0.762	
11	1.129	1.178	1.135	1.183	1.106	1.082	0.949	0.591	
	1.174	1.148	1.171	1.141	1.137	1.046	0.948	0.579	
	1.123	1.081	1.125	1.085	1.124	1.046	0.998	0.627	
	1.108	1.063	1.111	1.074	1.126	1.049	1.012	0.632	
12	1.168	1.126	1.177	1.106	1.202	0.881	0.842		
	1.128	1.154	1.127	1.137	1.166	0.961	0.832		
	1.071	1.120	1.079	1.124	1.146	1.036	0.876		
	1.069	1.111	1.067	1.126	1.166	1.059	0.888		
13	1.078	1.132	1.118	1.082	0.881	0.854	0.579		
	1.106	1.085	1.113	1.046	0.961	0.910	0.593		
	1.107	1.064	1.107	1.046	1.036	0.988	0.647		
	1.107	1.059	1.105	1.049	1.059	1.015	0.658		
14	1.009	1.000	0.999	0.949	0.842	0.579			
	0.977	1.022	0.952	0.948	0.832	0.593			
	0.999	1.076	0.972	0.998	0.876	0.647			
	1.003	1.089	0.976	1.012	0.888	0.658			
15	0.722	0.798	0.716	0.591					
	0.721	0.768	0.699	0.579					
	0.783	0.811	0.754	0.627					
	0.793	0.819	0.762	0.632					

Fig. 14. Normalized radial assembly power distribution at different burnup points.

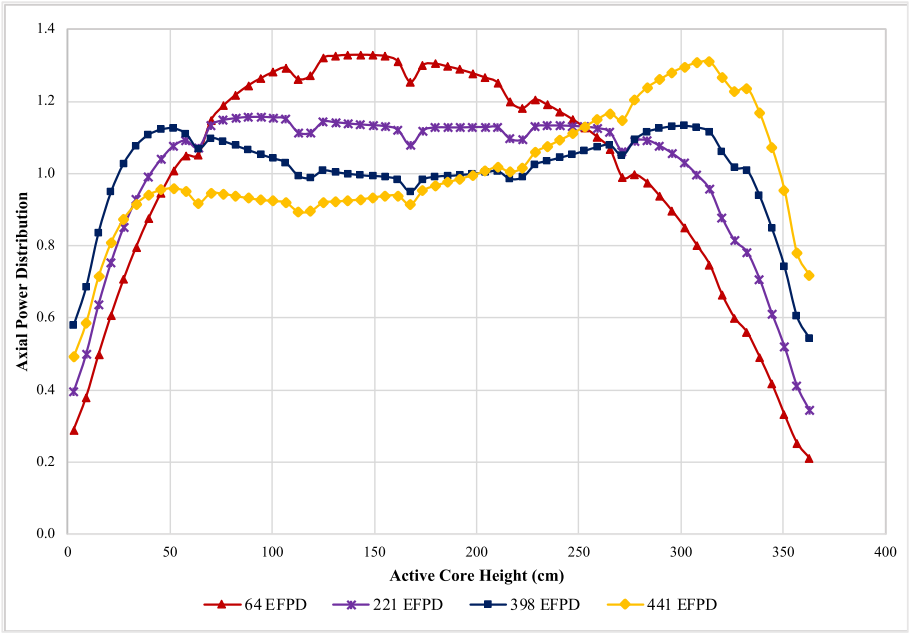

Fig. 15. 1D core axial power distribution at different burnup points.

and axial offset during the fuel cycle are shown in Fig. 17. Axial Offset (AO) fluctuated within a range of approximately −10%–10%. The sign of AO shifts from negative to positive due to a shift in power distribution along the axial direction throughout the fuel cycle.

5. Conclusion

Exercise 1 includes a range of Zero Power Physics Tests (ZPPT) problems taken from WB1C1, encompassing criticality tests, Control Rod Worth (CRW) calculations, ITC, and DBW calculations. There is strong agreement in all the presented scenarios. The criticality test

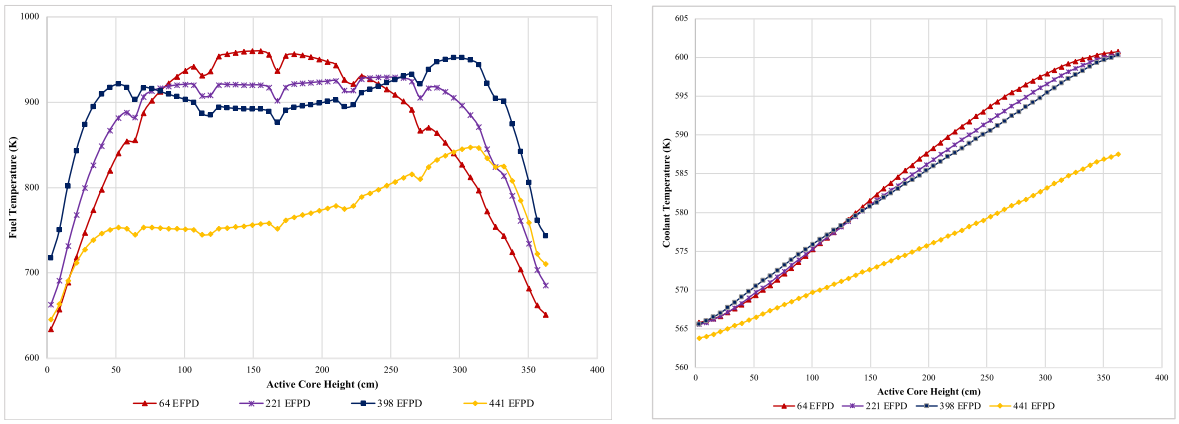

(a) Fuel Temperature Profiles (b) Coolant Temperature Profile

Fig. 16. 1D core axial fuel (a) and coolant (b) temperature at different burnup points.

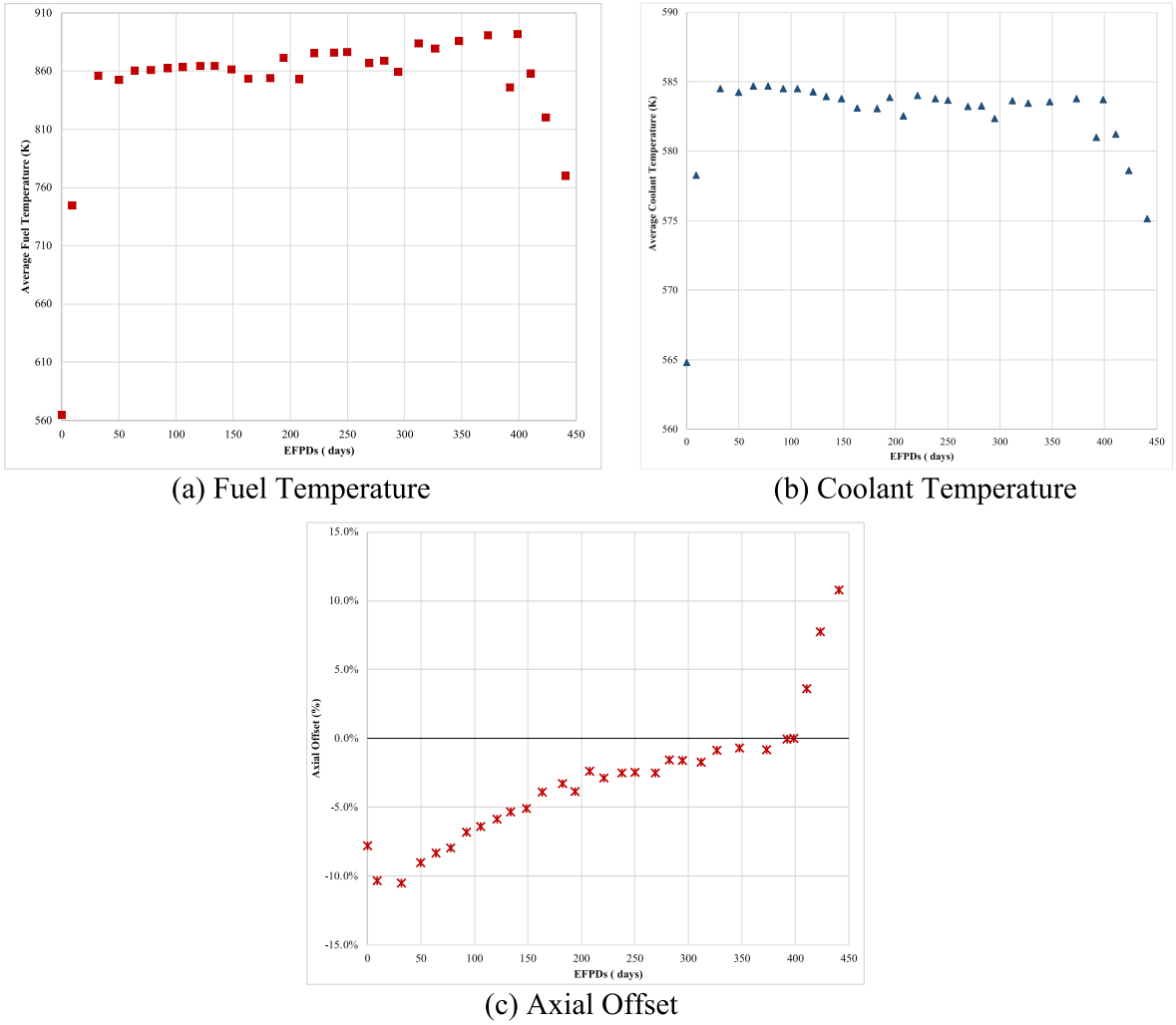

(a) Fuel Temperature (b) Coolant Temperature

(c) Axial Offset

Fig. 17. WB1C1 average temperature and axial offset profiles with ST3D: (a) Average fuel temperature, (b) average coolant temperature, and (c) axial offset (AO).

discrepancies consistently remain within a narrow margin of 130 pcm when compared to KENO-VI. In the case of CRW, the differences for each control bank are within the range of 0–60 pcm when compared to measured data and within 0–4 pcm when compared to KENO-VI. The ITC and DBW values of ST3D agree well with differences of −1.17 pcm/F and −0.56 ppm/pcm, respectively, when compared to KENO-VI. Additionally, a comparison of the radial and 1D core axial power profiles for the criticality case demonstrates a strong agreement with KENO-VI, yielding Root Mean Square (RMS) errors of 0.36% and 0.74%, respectively. Exercise 2 aims to analyze steady state multi-physics parameters at WB1C1 under normal operating conditions. CBC from ST3D-TH1D closely matches the results from MC21-CTF, with only a 4.1 ppm

difference. The RMS error for the normalized power distribution in the assembly is merely 0.42%, and the relative error for all fuel assemblies is less than 1%, indicating a strong agreement. Exercise 3 focuses on the prediction of WB1C1 fuel depletion, burnable absorbers, and the estimation of CBC values throughout the fuel cycle. Due to a lack of available data in the literature, only CBC values during the depletion cycle were compared in this section. ST3D demonstrates good consistency compared to plant-measured data. Additionally, average fuel and coolant temperature profiles, along with axial offset, are presented for the entire fuel cycle. Furthermore, 1D core axial power and temperature profiles are provided for four different burnup points. STREAM3D shows its capability to generate high-fidelity results for practical PWR core calculations.

Declaration of competing interest

The authors declare that they have no known competing financial interests or personal relationships that could have appeared to influence the work reported in this paper.

Acknowledgments

This work was partially supported by Korea Hydro & Nuclear Power Co. Ltd. (No. 2022-Tech-13). This work was partially supported by the Korea Institute of Energy Technology Evaluation and Planning (KETEP) and the Ministry of Trade, Industry & Energy (MOTIE) of the Republic of Korea (No. 20217810100050).

References

[1] Consortium for Advanced Simulation of Light Water Reactors (CASL), 2014. http://www.casl.gov.
[2] A.T. Godfrey, VERA core physics benchmark progression problem specifications. Consortium for Advanced Simulation of LWRs, 2014.
[3] T. Albagami, P. Rouxelin, A. Abarca, D. Holler, L. Moloko, M. Avramova, K. Ivanov, A. Godfrey, S. Palmtag, TVA Watts Bar Unit 1 Multi-Physics Multi-Cycle Depletion Benchmark Version 2.3.3, Technical Report NEA/EGMPEBV/DOC, 2022. The Organization for Economic Cooperation and Development (OECD) Nuclear Energy Agency (NEA) 2022.
[4] S. Choi, D. Lee, Three-dimensional method of characteristics/diamond-difference transport analysis method in STREAM for whole-core neutron transport calculation, Comput. Phys. Commun. 260 (2021) 107332.
[5] H.G. Joo, J.Y. Cho, K.S. Kim, C.C. Lee, S.Q. Zee, Methods and performance of a three-dimensional whole-core transport code DeCART, Proc. Physor (2004).
[6] B. Collins, S. Stimpson, B.W. Kelley, M.T. Young, B. Kochunas, A. Graham, E. W. Larsen, T. Downar, A. Godfrey, Stability and accuracy of 3D neutron transport simulations using the 2D/1D method in MPACT, J. Comput. Phys. 326 (2016) 612–628.
[7] M. Ryu, Y.S. Jung, H.H. Cho, H.G. Joo, Solution of the BEAVRS benchmark using the nTRACER direct whole core calculation code, J. Nucl. Sci. Technol. 52 (7–8) (2015) 961–969.
[8] W. Boyd, S. Shaner, L. Li, B. Forget, K. Smith, The OpenMOC method of characteristics neutral particle transport code, Ann. Nucl. Energy 68 (2014) 43–52.
[9] B.N. Aviles, D.J. Kelly, D.L. Aumiller, D.F. Gill, B.W. Siebert, A.T. Godfrey, B. S. Collins, R.K. Salko, MC21/COBRA-IE and VERA-CS multiphysics solutions to VERA core physics benchmark problem #6, Prog. Nucl. Energy 101 (2017) 338–351.
[10] M.E. Dunn, C. Bentley, S. Goluoglu, L.S. Paschal, L. Petrie, H. Dodds, Development of a continuous energy version of KENO Va, Nucl. Technol. 119 (3) (1997) 306–313.
[11] D. Griesheimer, D. Gill, B. Nease, T. Sutton, M. Stedry, P. Dobreff, D. Carpenter, T. Trumbull, E. Caro, H. Joo, MC21 v. 6.0–A continuous-energy Monte Carlo particle transport code with integrated reactor feedback capabilities. SNA+ MC 2013-Joint International Conference on Supercomputing in Nuclear Applications+ Monte Carlo, EDP Sciences, 2014 06008.
[12] H. Lee, W. Kim, P. Zhang, M. Lemaire, A. Khassenov, J. Yu, Y. Jo, J. Park, D. Lee, MCS–A Monte Carlo particle transport code for large-scale power reactor analysis, Ann. Nucl. Energy 139 (2020) 107276.
[13] S. Choi, C. Lee, D. Lee, Resonance treatment using pin-based pointwise energy slowing-down method, J. Comput. Phys. 330 (2017) 134–155.
[14] S. Choi, K. Smith, H.C. Lee, D. Lee, Impact of inflow transport approximation on light water reactor analysis, J. Comput. Phys. 299 (2015) 352–373.
[15] T.D.C. Nguyen, H. Lee, S. Choi, D. Lee, MCS/TH1D analysis of VERA whole-core multi-cycle depletion problems, Ann. Nucl. Energy 139 (2020) 107271.
[16] B.T. Rearden, M.A. Jessee, SCALE Code System, Oak Ridge National Lab.(ORNL), Oak Ridge, TN (United States), 2018.
[17] R. Salko, A. Wysocki, T. Blyth, A. Toptan, J. Hu, V. Kumar, C. Dances, W. Dawn, Y. Sung, V. Kucukboyaci, CTF: a modernized, production-level, thermal hydraulic solver for the solution of industry-relevant challenge problems in pressurized water reactors, Nucl. Eng. Des. 397 (2022) 111927.
[18] Y. Zheng, S. Choi, D. Lee, A new approach to three-dimensional neutron transport solution based on the method of characteristics and linear axial approximation, J. Comput. Phys. 350 (2017) 25–44.